Review

Specific Refractory Gold Flotation and Bio-Oxidation Products: Research Overview

Richmond K. Asamoah

Minerals and Resource Engineering, Future Industries Institute, University of South Australia, Mawson Lakes, SA 5095, Australia; richmond.asamoah@unisa.edu.au

Abstract: This paper presents a research overview, reconciling key and useful case study findings, towards uncovering major causes of gold refractoriness and maximising extraction performance of specific gold flotation and bio-oxidation products. Through systematic investigation of the ore mineralogical and gold deportment properties, leaching mechanisms, and kinetic behaviour and pulp rheology, it was observed that the predominant cause of the poor extraction efficacy of one bio-oxidised product is the presence of recalcitrant sulphate minerals (e.g., jarosite and gypsum) produced during the oxidation process. This was followed by carbonaceous matter and other gangue minerals such as muscovite, quartz, and rutile. The underpining leaching mechanism and kinetics coupled with the pulp rheology were influenced by the feed mineralogy/chemistry, time, agitation/shear rate, interfacial chemistry, pH modifier type, and mechano-chemical activation. For instance, surface exposure of otherwise unavailable gold particles by mechano-chemical activation enhanced the gold leaching rate and yield. This work reflect the remarkable impact of subtle deposit feature changes on extraction performance.

Keywords: refractory gold ores; ore mineralogy; secondary minerals; rheology and leaching kinetics; mechano-chemical activation

1. Introduction

The economic significance of gold to the development of several nations (e.g., Australia, South Africa, USA, China, Canada, and Ghana), owing to its coveted qualities and unique applications, can be traced back to the dawn of civilization [1–6]. In a recent global gold mine reserve estimation [7], Australia hosts 16% of the world's total 56,700 t gold (Figure 1) worth AUD$ 542.48 billion, at gold price of AUD$ 1690/oz. With record high gold prices in 2020 (AUD$ 2670/oz), the 16% gold deposit represents a higher value of about AUD$ 857.05 billion. A number of developing countries (e.g., Ghana), blessed with gold deposits, have substantially achieved poverty alleviation by exploiting their gold reserves in an eco-friendly manner. Gold extraction continue to represent a major livelihood and economic support in recent time.

Currently, a greater percentage of gold is extracted from low grade, refractory gold ores, following depletion of most high grade deposits [8]. Increasing complexity of these refractory ores warrants improvement in our fundamental and applied knowledge underpinning sustainable, cost-effective, commercial gold extraction process and commodity production. Despite numerous reported studies on improved gold extraction (by cyanide leaching) from complex low grade ores [9–16], there is still a lack of fundamental knowledge and understanding on the interplay between refractory ore-specific primary and secondary mineral phases, solution chemistry, and the particle-solution interfacial species, particle interactions, and chemical/electrochemical reactions which underpin the mechanisms and kinetics of the leaching process. How these factors interact synergistically to produce fast kinetics and high gold recovery or antagonistically (e.g., low leach rate, passivation/encapsulation, poor gold recovery, and high reagent consumption) during alkaline cyanide leaching process is as yet not clearly established.

Country	Gold in Monetary Terms * billion AUD
Australia	542.48
Russia	476.90
South Africa	357.68
United States	178.84
Indonesia	178.84
Peru	166.92
Brazil	774.97
Canada	143.07
China	113.26
Uzbekistan	101.34
Mexico	83.46
Ghana	71.54
Papua New Guinea	71.54
Other Countries	119.23
Total	3380.06
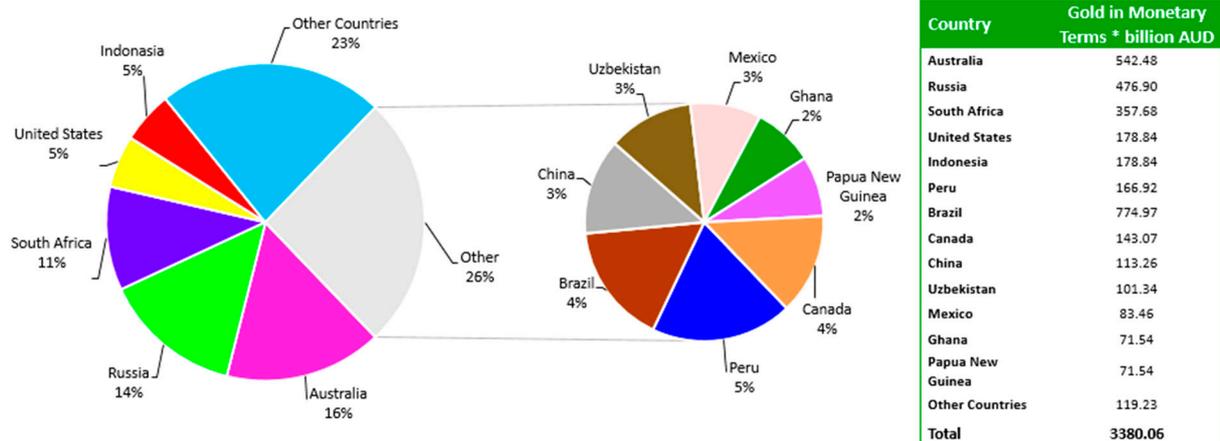
Figure 1. Global gold mine reserves in 2015. Total mine gold reserve was 56,700 metric tons whilst total monetary estimate was AUD$ 3380.06 billion [7].

Of relevance to the present work is a technological conundrum associated with gold extraction from two biologically oxidised (BIOX®) flotation concentrates obtained from the same low grade (<1.5 g/t) deposit (Ghana). Although the same process route and conditions are deployed for gold extraction, one bio-oxidised product invariably displayed ~20 wt.% lower gold recovery compared with the other (Figure 2). Furthermore, the cyanide leaching process typically requires low slurry solid loading (~35 wt.%) to facilitate pulp handleability. Nominally, 30–40 wt.% gold is lost to tailings upon alkaline cyanide leaching and simultaneous gold adsorption by activated carbon. In monetary terms, the gold lost to tailings is estimated to be AUD$ 5.7 million per annum for treating a low grade ore of 1 g/t at a 420 t/d plant throughput. In-plant studies based on extant literature review to understand the cause of refractoriness and poor pulp handleability were not conclusive due to the complexity of the ores and concentrates.
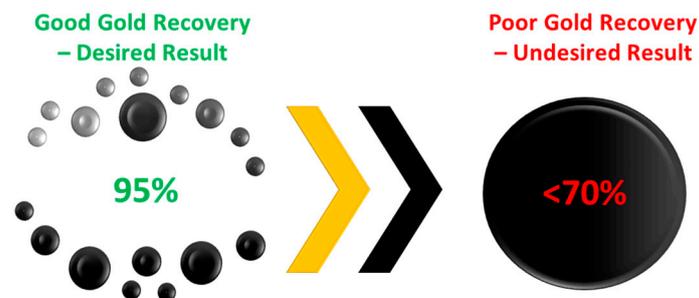
Figure 2. Specific gold extraction technological challenge for current work. Gold recovery reduced from 95% to <70%, leading to loss of about AUD$ 5.7 million per annum.

Overall, very limited mineralogical and chemical difference information between the lower and higher gold recovery bio-oxidised ores was available. There is paucity of knowledge of the relationship between the mineral processing and pre-treatment steps, pulp chemistry, process variables, and leaching kinetics and mechanism. The integrated occurrence of these issues rendered the processing plant unproductive, on the verge of closing down as the more easy-to-treat ores got depleted. For some mine operations, high grade leach tailings, due to gold loss during the leaching stage, are stockpiled with hope of reprocessing or sale. The lack of efficacious method represents significant waste of resources deployed in the extraction process. There is, therefore, a long-overdue need to bridge the knowledge gap and gain greater understanding of the leaching behaviour of such low grade, refractory gold ores through both strategic basic and applied studies.

In our previous papers, the ore mineralogical and physico-chemical characteristics, gold mineralisation and deportment in host gangue minerals, effect of selected process variables on the kinetics and mechanism of alkaline cyanide leaching and temporal rheological behaviour, and refractory attenuation capability of mechano-chemical activation technique have been investigated, attempting to address critical questions and aspects of poor process performance [17–23]. This paper, therefore, aims at

1. Reconciling and discussing all the key findings emerging from the comprehensive, investigations presented;
2. Determining the overall impact of process variables on the leaching behaviour and rheological behaviour; and
3. Summarise the different mechanisms and kinetics which underpin the leaching behaviour with links to extant literature.

This provides overarching discussions, highlighting how the new knowledge and greater understanding gleaned may be useful in designing ore mineralogy-specific, customised approach and strategies for improved, cost-effective gold extraction from complex, refractory, sulphidic ores.

2. Ore Mineralogy and Physico-Chemistry

Ore mineralogy coupled with physico-chemical characteristics play a critical role in their response to mineral processing and extraction techniques. The comprehensive mineralogy and physico-chemistry of the two different gold ores alongside their flotation and bio-oxidation products have been investigated. It was evident that the two gold ores comprise common minerals such as quartz, chamosite, albite, ephesite, clinozoisite, larnite, illite, muscovite, rutile, pyrite, arsenopyrite, apatite, dolomite, and siderite. The key difference observed of the two ores was the variation in the percentages of some common minerals.

The characteristic differences between the two ores reflected two types of flotation concentrates, uniquely distinguished by two different minerals. Arsenopyrite, muscovite, and pyrite were upgraded for the two flotation concentrates to different extents. One concentrate was predominated by dolomite (hereafter referred to as dolomite-containing flotation concentrate—DC) whilst the other was predominated by apatite (hereafter referred to as apatite-containing flotation concentrate—AC). Both dolomite and apatite were initially present in the two flotation feed ores, however, their variable, complex associations with other hydrophobic minerals defined their rejection or inclusion in the flotation concentrate. DC comprised more amount of hydrophobic, sulphide minerals than the AC which contained higher ephesite, illite, and albite as well. Quantitative Evaluation of Minerals by Scanning Electron Microscopy (QEMSCAN) investigation revealed smaller mineral grain size in AC compared with DC (Table 1). This observation agrees with the different mineral response of the two refractory gold ores to flotation.

Subsequent to bio-oxidation, AC yielded jarosite-containing bio-oxidation product (hereafter referred to as JC) with greater bassanite content whereas DC produced jarosite-free bio-oxidation product (hereafter referred to as JF) with bassanite and gypsum present in lower and higher amounts, respectively. This result agrees with some previous works [24–26] which showed that phosphate ions facilitate precipitation of jarosite at the typical bio-oxidation conditions (e.g., pH 1.0–1.8). Although phosphorus are required by the chemolithothrophic bacteria for oxidising the flotation concentrates, the amount added by the apatite-bearing flotation concentrates (7.3 kg/t) are by far more than prescribed BIOMIN rates of 0.9 kg/t. Table 2 shows the potassium and sodium content before and after bio-oxidation. Evidently, potassium and sodium was concentrated in the bio-oxidation products with little difference between JF and JC in terms of percentage of upgrade. A further studies will characterise the jarosite found in JC to determine whether it is H, Na, K or NH_4.

Table 1. Mineral mass (%) and average grain size (μm) of studied flotation and bio-oxidation products using QEMSCAN. Modified after Asamoah et al, 2019 [1]. DC—Dolomite containing flotation concentrate, AC—Apatite-containing flotation concentrate, JF—Jarosite-free bio-oxidised product, JC—Jarosite-containing bio-oxidised product.

Mineral Phases	Mineral Mass (%)				Average Grain Size (μm)			
	DC	AC	JF	JC	DC	AC	JF	JC
Pyrite	36.0	24.2	0.7	1.0	35.1	13.7	13.9	6.4
Arsenopyrite	7.5	5.0	0.1	0.1	11.2	8.6	6.9	5.9
Pyrrhotite	1.1	0.3	0.0	0.1	4.5	4.6	2.9	3.1
Other Sulphides	0.2	0.2	0.2	0.4	8.0	7.1	3.9	4.9
Quartz	17.1	27.3	35.7	33.3	16.2	9.8	9.1	10.4
Feldspar	4.0	4.6	4.9	5.1	13.2	8.4	8.7	8.8
Muscovite/Illite/Biotite	20.2	23.2	32.8	32.6	15.3	8.2	7.4	9.1
Other silicates (chlorites, amphibole, kaolinite, pyroxene)	6.2	7.9	7.1	5.7	4.3	4.7	3.9	3.7
Dolomite	5.2	0.8	0.0	0.0	14.0	9.6	3.7	5.5
Other Carbonates	0.1	0.1	0.1	0.2	4.6	4.2	5.8	5.2
Apatite	0.1	3.8	0.0	0.1	7.9	7.4	5.5	6.4
Rutile/Ilmenite	1.2	1.4	2.6	2.0	7.1	7.7	7.2	6.8
Magnetite/Hematite/Goethite	0.5	0.7	2.5	2.2	12.0	8.1	6.6	10.1
Jarosite	-	-	0.0	5.5	-	-	2.9	3.2
Anhydrite	-	-	13.1	11.5	-	-	20.9	18.6
Others	0.6	0.5	0.2	0.2	4.8	5.0	3.3	3.4

Table 2. Potassium and sodium content before and after bio-oxidation for samples AC and DC. 95% Confidence Interval.

Elements	Unit	DC	AC	JF	JC
K	%	1.2	1.6	2.1	2.0
Na		0.8	1.0	1.3	1.6

The percent sulphide–sulphur oxidation for JF was greater than that of JC. The mineral association results made evident by photomicrographs showed greater surface coating of unreacted and partially reacted sulphide minerals in JC than JF. The surface coating behaviour of the jarosite minerals attenuated the liberation of gold after the bio-oxidation for subsequent alkaline cyanide leaching. The observations were consistent with the sulphur speciation data.

The bulk chemistry data also showed that the concentration of gold in the refractory gold ore, before flotation, producing DC (~2.3 g/t) was more than that yielding AC (~1.3 g/t). The gold grade was increased by ~14 and ~15 times after flotation for DC and AC, respectively. Breakdown in the mineral structures after bio-oxidation led to ~1.4 times increase in the gold grade of both JF and JC. Surface chemistry investigations by EDTA extraction showed that jarosite minerals coated the surfaces of both soluble and insoluble minerals [20]. For instance, upon extracting the EDTA extractable iron species which were insoluble in water only, other soluble mineral phases (e.g., gypsum) were dissolved. Photomicrographs showing complex association between jarosite and gypsum confirmed the EDTA results [20]. Figure 3 shows a schematic diagram of the influential role of jarosite and gypsum following bio-oxidation. Evidently, subtle variations in the ore mineral occurrence and characteristics defined the mineral processing and pre-treatment product features which underpin downstream gold extraction performance.
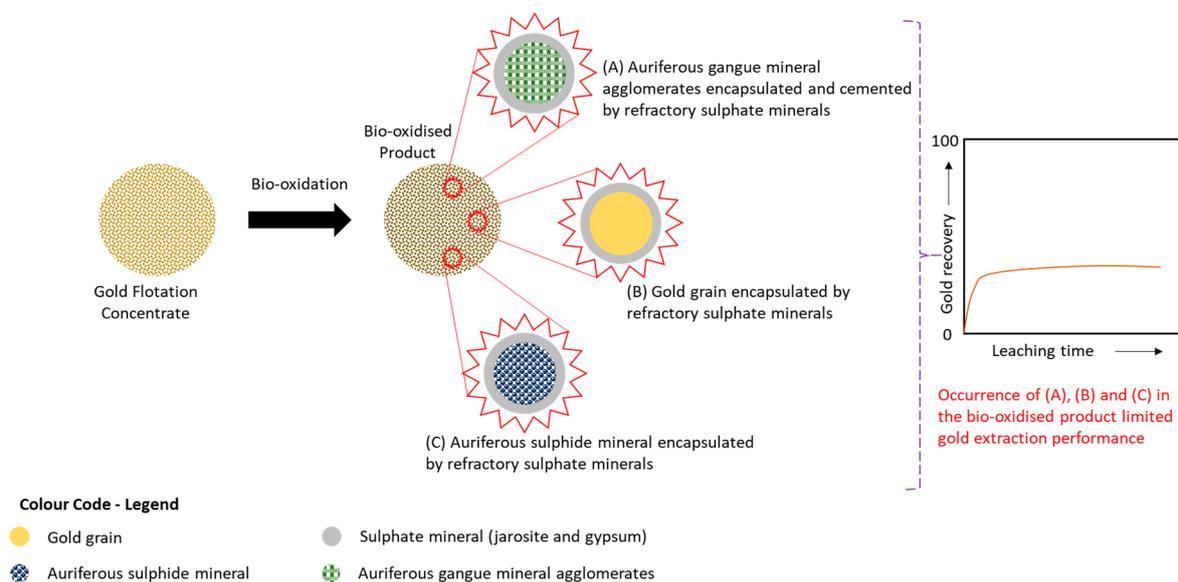
Figure 3. Schematic diagram showing the influential role of secondary sulphate minerals (gypsum, jarosite) formed after bio-oxidation on gangue minerals, auriferous sulphides, and gold grains.

Carbon speciation of the two ore types, before and after flotation and bio-oxidation, showed presence of graphitic, organic, and other inorganic (e.g., carbonate) carbons. The total carbon content also increased after flotation of the comminuted ores. Although statistically the same graphitic content was noted in the flotation concentrates, the graphitic content after bio-oxidation were more in JF compared with JC. On the contrary, the organic carbon content of JC was greater than that of JF, suggesting that the organic carbon was acid-soluble. Studies on the preg-robbing capacity of the bio-oxidation products showed

greater values for JF than JC. This was confirmed by spectroscopic studies which also showed greater Raman ratio for JF (1.1) than JC (0.8). The higher the Raman ratio, the greater the gold preg-robbing capability of the ore. The lower gold absorption capability of the graphitic carbon in JC may be due to possible surface coatings on adsorption sites.

The flotation concentrates and bio-oxidised products' particle size distribution showed two different trends after bio-oxidation. Whilst the DC and AC showed particle size distribution, the JF and JC showed finer and coarser particle sizes, respectively. The breakdown of mineral structure during bio-oxidation suggests reduction in the particle size as observed between DC and JF. The increase in the particle size after bio-oxidation of AC was due to the formation of jarosite minerals which facilitated ore particle agglomeration [27,28].

In addition, the particle specific surface area of AC was greater than that of DC. These data indicated greater porosity of the AC than DC. After bio-oxidation, however, the formation of jarosite minerals on the surfaces of porous gangue minerals and the attenuation of sulphide oxidation led to a lower specific surface area in JC compared with the flotation concentrate feed and JF, contrary to expectations.

It is worth mentioning that the processing plant from which the samples were derived initially treat an apatite-free flotation concentrate (e.g., dolomite-containing concentrates—DC) and hence no jarosite is observed in their bio-oxidised products. Emergence of the complex associated, AC feed ores under equal processing strategies yielded deleterious jarosite phases, impacting the bio-oxidised product mineralogy, and physico-chemistry.

3. Gold Mineralisation and Deportment

The mine that provided the samples nominally observes that the jarosite-bearing bio-oxidised product (~70 wt.%) invariably display lower gold recovery relative to the jarosite-free bio-oxidised product (~90 wt.%) after 24 h of carbon-in-leach. The mineralogical and physico-chemical characteristics showed differences in the products following flotation and bio-oxidation which could be responsible for gold refractoriness and the lower gold recovery noted for JC. It was, however, crucial to obtain a quantitative information on the percent of cyanide-insusceptible gold for extraction due to a given ore-specific cause of refractoriness.

Both visible and invisible gold occurred in the flotation concentrates and bio-oxidation products. Invisible gold particles include solid solution and nano-sized gold grain in gangue mineral hosts such as arsenopyrite and pyrite. The average visible gold grain size and distribution data of the flotation concentrates, and bio-oxidation products, showed presence of coarser gold grains in AC and JF compared with DC and JF, respectively. Sample JF showed gold grain size range of 0.2 to 20.7 μm whilst that of JC was 0.1 to 30.6 μm. This observation also makes evident the key differences between the two refractory gold ores. Although they both originate from a common deposit, the gold grain sizes are significantly different and hence may display different leaching trends even if all the gold particles were liberated and available.

Liberation and locking statistics data from QEMSCAN analysis showed that all the gold particles in the flotation concentrates displayed liberation <10%. However, after bio-oxidation, the liberation of the gold particles improved in an ore-specific manner. The JF showed ~90% gold liberation to be <10% with the remaining ~10% being for <20% to 100% gold liberation. JC, on the other hand, showed ~8% gold displaying <10 liberation, with the remaining ~92% occurring between <20% and 100% liberation. Generally, this observation suggests higher leaching of gold in JC than JF, notwithstanding, a factor not included in above statistics is invisible gold.

A very important factor worth considering, however, is the gold grain sizes between the two products and the limitation of the technique deployed. Thus, the gold grain sizes in the JC are greater than JF. Further, the QEMSCAN is unable to detect submicron gold particles and submicron surface coatings. Consequently, very fine gold particles that may be liberated in JF would not be detected and appropriately discriminated based on their liberation status. Similarly, submicron gold surface coatings or encapsulation which may

exist in JC cannot be identified by QEMSCAN. All such particles will be therefore reported as liberated.

The QEMSCAN investigation revealed that visible gold particles found in DC were associated with arsenopyrite, pyrrhotite, muscovite, galena, pyrite, chalcocite, digenite, sphalerite, illite, biotite, feldspar, magnetite, geothite hematite, and rutile. AC also showed similar gold associations coupled with gold-quartz association. Overall, the two flotation concentrates showed greater association between the visible gold particles and arsenopyrite. Unlike the flotation concentrates, greater amount of the visible gold particles, observed in JF, were in association with pyrite whilst those of JC were in association with arsenopyrite.

The greater gold-pyrite association in JF, despite the higher gold-arsenopyrite association in its corresponding flotation concentrate (DC) is consistent with the literature [29]. For instance, it is well known that bio-oxidation is more effective in oxidising arsenopyrite minerals which display ease for oxidation by the chemolithotrophic bacteria. On the contrary, the observed greater gold-arsenopyrite association in JC confirms the sulphur speciation results which showed poor sulphide-sulphur oxidation evidenced by the surface coated, sulphide mineral, and photomicrographs [20]. Poor arsenopyrite oxidation prevented the release of gold particles in their unoxidised mineral matrix.

Furthermore, gold particles were hosted by agglomerates of gangue minerals (e.g., pyrite, monazite, muscovite, and quartz) that were noted in the jarosite-bearing bio-oxidised product [21]. Backscattered electron (BSE)/energy dispersive X-ray (EDX) investigations revealed that some visible gold were encapsulated by sulphate minerals in the bio-oxidised products. Whilst gold encapsulation by gypsum and jarosite were noticeable in JC, only gypsum encapsulation of gold was noticeable in JF. The observed gold coatings thickness was variable; however, finer surface coatings were noticeable in JC. In addition, the invisible gold were mostly hosted by arsenopyrite and arsenian pyrite minerals. The solid-solution gold was more pronounced than the nano-sized gold particles that were hosted by the gangue minerals. Arsenopyrite minerals hosted majority of the invisible gold grains. The gold concentration in the arsenian pyrite was defined by the concentration of arsenic. As the arsenic content increased in the pyrite mineral, so did the invisible gold content. The invisible gold content of DC was more pronounced compared with AC. This further shows that most of the gold particles that were liberated from DC after bio-oxidation (JF) were invisible that cannot be detected by the QEMSCAN method of analysis. These complex associations and causes of refractoriness warranted the study of gold deportment per mineral group in the flotation concentrates and the bio-oxidised products.

Gold deportment studies, using diagnostic leaching, showed that after cyanidation of the flotation concentrates and bio-oxidation products, ~79 and ~77 wt.% of gold in DC and AC were, respectively, unextractable. On the other hand, ~31 wt.% and ~78 wt.% of gold in JF and JC were unrecovered by cyanide leaching. The sulphide minerals are the major cause of refractoriness in the flotation concentrates. For the bio-oxidation products, different dominant refractory causing components were observed between the two samples. JF showed carbonacoues matter as the major cause of refractoriness whilst JC showed sulphate minerals as the major cause of refractoriness.

JF and JC comprised both gypsym and bassanite minerals; however, the presence of jarosite was exclusive to AC only. The negative secondary sulphate mineral impact could therefore be ascribed to the jarosite minerals that were associated with JC only. The jarosite minerals may have encapsulated the gold particles completely or partially where other gangue minerals are also in association with gold. Partial removal of the jarosite minerals could enhance galvanic leaching of gold particles that are in association with minerals with higher rest potentials (e.g., galena).

Although the refractory causing behaviour in JF, where the major cause of refractoriness is the presence of carbonaceous matter, is well documented in literature, those associated with JC, showing secondary sulphate minerals such as jarosite as the main cause of refractoriness is now known. Figure 4 illustrates the various gold occurrences in the investigated flotation concentrates and bio-oxidation products. The gold extraction

limiting potential of the jarosite phases could reflect significant losses in mine productivity and sustainability.
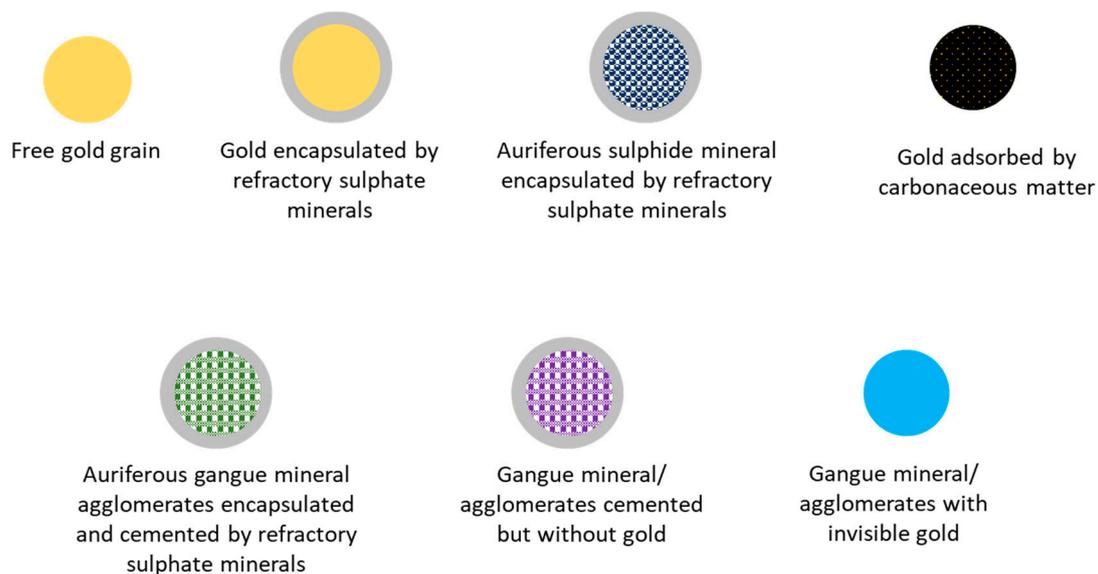
Figure 4. Illustration of the occurrence of gold in the investigated flotation concentrates and bio-oxidation products.

4. Effect of Process Variables on Cyanide Leaching Mechanism and Kinetics

The effect of process variables (e.g., mineralogy, time, agitation rate, and pH modifier) on the mechanism and kinetics of batch isothermal leaching cyanide susceptible gold from the flotation concentrates and bio-oxidised products was investigated.

Cyanidation of the flotation concentrates did not show noticeable variation in feed ore mineralogy and chemistry (except gold content), irrespective of the pH conditioner type. In case of the bio-oxidised products, however, pronounced mineralogy changes were evident when caustic soda was used. Bassanite and gypsum minerals which are usually soluble in aqueous solution leached out from JF following 8 h of cyanidation using sodium hydroxide as pH conditioner. When quicklime was deployed, only gypsum was dissolved from JF following 8 h of cyanidation. The results showed gypsum as refractory in JC alongside jarosite. This observation is consistent with the complex jarosite–gypsum association observed in the product.

In addition to shear-induced breakage of gangue mineral agglomerates which was more evident in the jarosite-bearing bio-oxidised product, the particle size distribution of all leach feeds and ripios were substantially the same. Brunner-Emmett-Teller (BET) specific surface area results were the same for the flotation concentrates, irrespective of the pH conditioner used and their variable mineralogy. On the contrary, the bio-oxidation products showed increase in specific surface area when sodium hydroxide was used in conditioning the pH. For quicklime conditioned pulps, no variations were noted between the BET surface area of the leach feeds and ripios.

Ore mineralogy, leaching time, and pH modifier-dependent gold leaching behaviour was observed during cyanidation of the flotation concentrates and bio-oxidation products. Within the initial 30 min of leaching, relatively rapid gold leaching rates were noted for the flotation concentrates and bio-oxidised products, irrespective of pH conditioner type and feed ore mineralogy. The first 30 min leaching rates for flotation concentrates was approximately six orders of magnitude lesser compared with leaching rates reported for some sulphide ores (Table 3). Similarly, about three to four orders of magnitude lesser leaching rates were noticeable for the bio-oxidised products when compared with roast-oxidised gold ores.

Table 3. Gold leaching rate comparison for selected studies.

Reference	Gold Leaching Rate ($mol \cdot m^{-2} \cdot s^{-1}$)	Agitation Rate (rpm)	pH Modifier	Leaching Time (min)	Gold Sample
Cathro and Koch [30]	5.52×10^{-5}	-	-	-	Pure gold
Lorenzen [31]	6.27×10^{-6}	Not specified	Caustic potash	0–150	Pure gold
Aghamirian and Yen [32]	8.50×10^{-6}	500	Caustic soda	0–140	Pure gold
Dai and Jeffrey [33]	5.6×10^{-5}	300	Caustic soda	0–180	Pure gold
Azizi et. al., [34]	6.6×10^{-6}	500	Caustic soda	0–60	Sulphide gold ore
Azizi et. al., [34]	2.16×10^{-5}	500	Caustic soda	0–60	Electro-oxidised gold ore
Bas et. al., [35]	5.3×10^{-8}	100	Caustic soda	0–180	Roast-oxidised gold ore
Asamoah et. al., [17]	3.34×10^{-12} 3.52×10^{-12}	600 1000	Caustic soda	0–30	Dolomite-bearing flotation concentrate
	1.02×10^{-12}	600	Quicklime		
	1.28×10^{-12} 1.35×10^{-12}	600 1000	Caustic soda		Apatite-bearing flotation concentrate
	8.13×10^{-12}	600	Quicklime		
	8.10×10^{-12} 1.18×10^{-11}	600 1000	Caustic soda		Jarosite-free bio-oxidised product
	3.62×10^{-12}	600	Quicklime		
	2.02×10^{-12} 8.03×10^{-12}	600 1000	Caustic soda		Jarosite-bearing bio-oxidised product

Although the overall gold leaching rates and yield from the flotation concentrates and bio-oxidised products reduced with modifying the pulp using quicklime in place of sodium hydroxide, there are some pulp conditions, defined by the ore mineralogy/chemistry, which favours the initial leaching rates (e.g., within 30 min) of quicklime modified pulps. This observation is more noticeable for JC. It was evident that within the initial 30 min, positive redox potentials occurred in the quicklime modified pulps whilst negative redox potential was observed in the sodium hydroxide modified pulp for the jarosite-bearing bio-oxidised product. The positive redox potential enhanced the gold leaching rate, and hence the observed higher leaching rates for the quicklime relative to sodium hydroxide. Calcium-oxide species deposition on pure gold particle was also noticeable in the quicklime conditioned pulps.

Furthermore, higher agitation rates did not have a significant effect on the gold leaching behaviour of the flotation concentrate. On the contrary, the leaching rates of the bio-oxidised products improved with higher agitation rates. The lack of influence of agitation rate on the flotation concentrate leaching behaviour suggests that the major rate determining step did not involve volume diffusion of lixiviant and reaction products to, and from the reaction sites, respectively. For the bio-oxidised products, however, diffusion of lixiviant and reaction products within porous layers which evolved around the gold containing minerals played a very key role in the leaching kinetics.

Modelling of the cyanidation mechanism and kinetics revealed that the flotation concentrates was chemical reaction controlled, shrinking core model whilst the bio-oxidised products followed diffusion through porous layer controlled, shrinking core model, both in a two stage manner. The two stage best-fit manner is ascribed to the initial rapid cyanidation of liberated gold followed by latter slow leaching of more refractory gold minerals. Good correlation of the predicted and actual gold recovery confirmed the model adequacy in predicting the gold leaching behaviour.

5. Temporal Rheological Behaviour: Effect of Mineralogy and Pulp-Interfacial Chemistry

The effect of mineralogy and pulp chemistry coupled with interfacial in rheological behaviour of the flotation concentrates and bio-oxidation products during cyanidation has been investigated. It was evident that variation in the mineralogy, interfacial chemistry and pulp chemistry played a subtle role on the rheology of the flotation concentrates. In addition, the flotation concentrates displayed a time-independent rheological behaviour. For the bio-oxidised products, ore mineralogy, physiology, pulp chemistry (pH modifier type), interfacial chemistry, and time-based rheological behaviour was noticeable.

In case of sodium hydroxide conditioned, JF pulps, reduction in rheology was observed for the first 60 min followed by accentuation of the pulp rheology to the initial state. For JC, on the other hand, weakening of the pulp rheology was generally observed without reverting to initial state at the end of the experiment. The continuous weakening in the pulp rheology of JC was attributed to its physiological nature. For instance, disintegration of the gangue mineral agglomerates, as evidenced by the particle size mean diameter, weakened the inter-particle attractive forces.

Generally, introduction of calcium ions in the form of quicklime displayed significant impact on the interfacial chemistry and pulp rheology. Interfacial chemical studies revealed that using quicklime rather than sodium hydroxide fostered particle charge reversal and screening as a result of the electropositive, hydrolysed calcium species adsorption together with $Ca(OH)_2{}^0$ surface nucleation. This observation was consistent with the Ca-O coating on pure gold substrate. The magnitude of the calcium species, zeta potential screening action was also defined by the ore mineralogy.

The metal ions-mediated shear rheology enhancement is attributed to the Ca(II) ion specific adsorption onto particles. These adsorbed ions and/or their hydrolysis products which partially or incompletely cover the surfaces of particles, enhance the interparticle attraction. A combination of non-DLVO attractive force mechanisms, defining the observation, may be the major cause of the observed poor handleability (Figure 5).
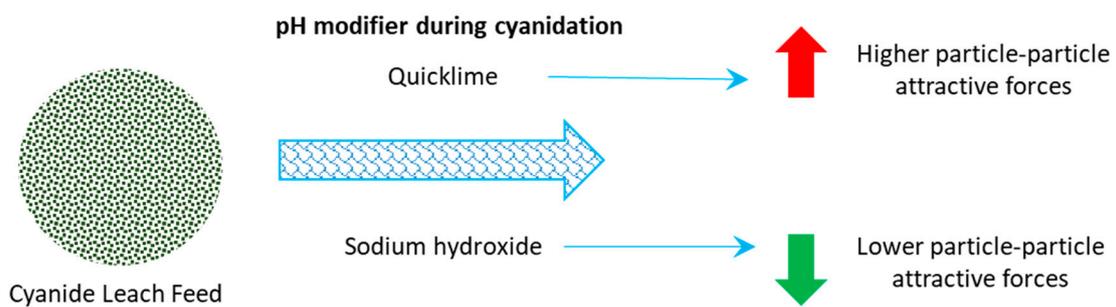
Figure 5. Illustration of the effect of pH modifier type on the particle-particle interaction during cyanidation.

6. Mechano-Chemical Activation of Bio-Oxidation Product: Leaching Behaviour
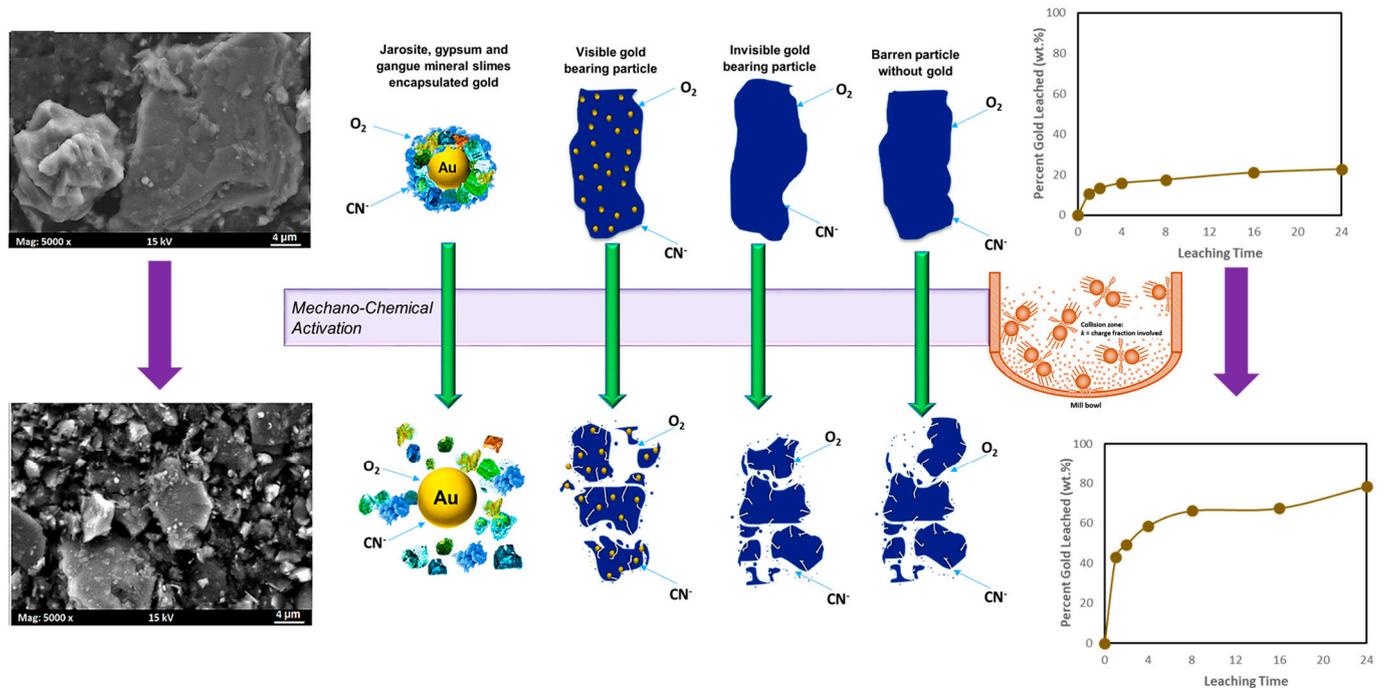
Mechano-chemical activation of the more refractory jarosite-bearing bio-oxidised product showed notable particle size reduction and corresponding increase in BET specific surface area. Greater activation parameters (milling time, milling speed, and ball to pulp ratio) magnitudes further lowered the particle size whilst increasing the specific surface area and relative amorphous content. Refractory gypsum minerals in the bio-oxidised product became soluble following mechano-chemical activation. On the other hand, portions of rutile, jarosite, goethite, quartz, albite, chamosite, and ephesite were transformed to amorphous. Furthermore, gangue mineral agglomerates, present in JC, were disintegrated with the level of breakage increasing with the mechanical stress deployed. Leaching behaviour of the activated feeds showed an increased in the gold leaching rates and yield. Overall, ~1.8 times higher gold recovery, following 24 h leaching of the 20 min mechano-chemically activated product, was observed to be maximum yield (Figure 6).
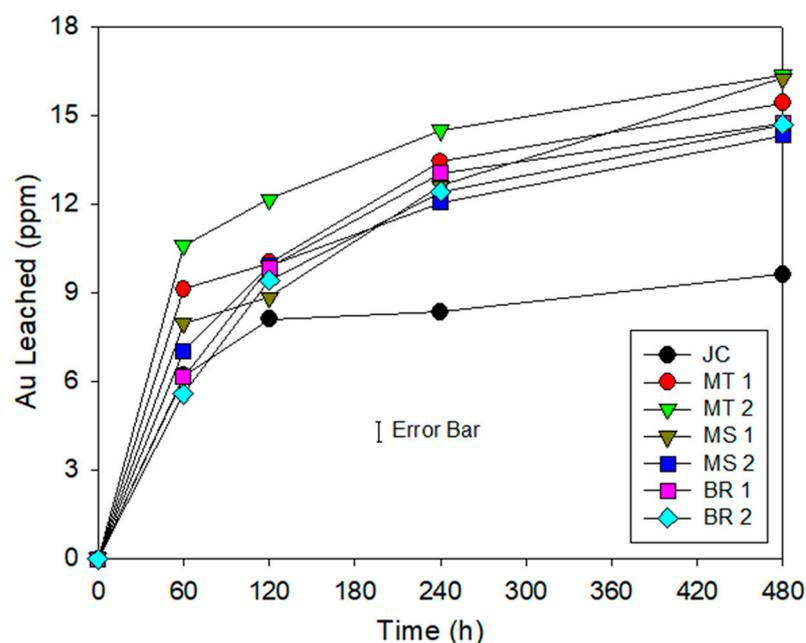
Figure 6. As-received (JC) and mechano-chemically activated JC gold leaching behaviour as a function of time. The mechano-chemically activated samples include those obtained from 5 min (MT1) and 20 min (MT2) milling time; 600 rpm (MS1) and 800 rpm (MS2) milling speed; and ball to pulp ratio of 5:1 (BR1) and 10:1 (BR2). For a given experiment, all other parameters are kept constant as follows: milling time—10 min; milling speed—1000 rpm; and ball to pulp ratio—2:1.

Furthermore, it was evident that the increase in gold leaching rate and recovery following mechano-chemical activation was independent on excessive increase in mechanical stress leading to very small particle sizes, high BET surface area, and mineral disordering.

On the contrary, the increase in gold leaching rate and recovery was defined by the disintegration of gold-gangue mineral agglomerates, surface cleaning of passivated gold particles and pore formation enabling gold site access within gangue minerals (Figure 7).

Figure 7. Schematic diagram showing the effect of mechano-chemical activation on the refractory bio-oxidation product and gold extraction performance, Modified after Asamoah et al. 2018 [18].

7. Conclusions

Subtle deposit feature changes can reflect notable effect on gold extraction performance, leading to inconsistent and in some cases uneconomical gold extraction. In this paper, a research overview, reconciling key and useful case study findings, have been presented in unravelling the major causes of gold refractoriness and maximizing specific gold extraction performance. Evidently, the major cause of gold refractoriness in the obstinate ore was the presence of refractory secondary sulphate minerals (e.g., gypsum and jarosite). Otherwise, both investigated ore types showed the effect of carbonaceous matter and other gangue minerals on gold extraction performance. The bio-oxidation product leaching mechanism and kinetics together with rheological behaviour were influenced by the feed mineralogy/chemistry, time, agitation/shear rate, interfacial chemistry, pH modifier type and mechano-chemical activation. Mechano-chemical activation of the refractory bio-oxidation product aided in overcoming the sulphate mineral-imposed refractoriness and improved gold recovery by about 1.8 times. Better monitoring of subtle process changes could help minimize process instabilities and maximize financial performance of mine operations.

Institutional Review Board Statement: Not applicable.

Informed Consent Statement: Not applicable.

Data Availability Statement: Not applicable.

Conflicts of Interest: There is no conflict of interest for this work.

References

1. Viewing, K.A. Gold '82: The Geology, Geochemistry and Genesis of Gold Deposits. In Proceedings of the Symposium Gold '82, University of Zimbabwe, Harare, Zimbabwe, 24–28 May 1982; A. A. Balkema: Rotterdam, The Netherlands, 1984.
2. Webber, K. *Australian Gold Rush: Gold Fever*; Macmillan Publishers Australia: Sydney, NSW, Australia, 2012; p. 32.
3. Corti, C.; Holliday, R. *Gold: Science and Applications*; CRC Press, Taylor and Francis Group: Boca Raton, FL, USA, 2010; p. 444.
4. Habashi, F. Gold—An Historical Introduction. In *Gold Ore Processing: Project Development and Operations*; Adams, M.D., Ed.; Elsevier: Amsterdam, The Netherlands, 2016; pp. 1–20.
5. Hontanilla, B.; Marre, D. Eyelid Reanimation with Gold weight implant and tendon sling suspension: Evaluation of excursion and velocity using the FACIAL CLIMA system. *J. Plast. Reconstr. Aesthet. Surg.* **2013**, *66*, 518–524. [CrossRef] [PubMed]
6. Lee, S.-M.; Kim, H.J.; Ha, Y.J.; Park, Y.N.; Lee, S.K.; Park, Y.B.; Yoo, K.H. Targeted chemo-photothermal treatments of rheumatoid arthritis using gold half-shell multifunctional nanoparticles. *ACS Nano* **2013**, *7*, 50–57. [CrossRef] [PubMed]
7. Statista. World Mine Reserve of Gold as of 2015, by Country. Mining, Metals and Minerals. 2016. Available online: http://www.statista.com/statistics/248991/world-mine-reserves-of-gold-by-country/ (accessed on 23 June 2016).
8. Adams, M.D. *Gold Ore Processing: Project Development and Operations*; Elsevier: Amsterdam, The Netherlands, 2016; Volume 15.
9. Bas, A.D.; Ghali, E.; Choi, Y. A review on electrochemical dissolution and passivation of gold during cyanidation in presence of sulphides and oxides. *Hydrometallurgy* **2017**, *172*, 30–44. [CrossRef]
10. Deschênes, G. Advances in the cyanidation of gold. In *Gold Ore Processing—Project Development and Operations*; Adam, M.D., Ed.; Elsevier: Amsterdam, The Netherlands, 2016; pp. 429–445.
11. Fomchenko, N.V.; Kondrat'eva, T.F.; Muravyov, M.I. A new concept of the biohydrometallurgical technology for gold recovery from refractory sulfide concentrates. *Hydrometallurgy* **2016**, *164*, 78–82. [CrossRef]
12. Li, Q.; Zhang, Y.; Li, X.; Xu, B.; Yang, Y.; Jiang, T.; Li, H. Intensification of gold leaching from a multi-refractory gold concentrate by the two-stage roasting—Alkaline sulfide washing—Cyanidation process. In *8th International Symposium on High-Temperature Metallurgical Processing*; Springer: Berlin, Germany, 2017.
13. Mubarok, M.Z.; Winarko, R.; Chaerun, S.K.; Rizki, I.N.; Ichlas, Z.T. Improving gold recovery from refractory gold ores through biooxidation using iron-sulfur-oxidizing/sulfur-oxidizing mixotrophic bacteria. *Hydrometallurgy* **2017**, *168*, 69–75. [CrossRef]
14. Nunan, T.O.; Viana, I.L.; Peixoto, G.C.; Ernesto, H.; Verster, D.M.; Pereira, J.H.; Teixeira LA, C. Improvements in gold ore cyanidation by pre-oxidation with hydrogen peroxide. *Miner. Eng.* **2017**, *108*, 67–70. [CrossRef]
15. Ofori-Sarpong, G.; Osseo-Asare, K.; Tien, M. Mycohydrometallurgy: Biotransformation of double refractory gold ores by the fungus, Phanerochaete chrysosporium. *Hydrometallurgy* **2013**, *137*, 38–44. [CrossRef]
16. Oraby, E.A.; Eksteen, J.J.; Tanda, B.C. Gold and copper leaching from gold-copper ores and concentrates using a synergistic lixiviant mixture of glycine and cyanide. *Hydrometallurgy* **2017**, *169*, 339–345. [CrossRef]
17. Asamoah, R.K.; Skinner, W.; Addai-Mensah, J. Alkaline cyanide leaching of refractory gold flotation concentrates and bio-oxidised products: The effect of process variables. *Hydrometallurgy* **2018**, *179*, 79–93. [CrossRef]
18. Asamoah, R.K.; Skinner, W.; Addai-Mensah, J. Leaching behaviour of mechano-chemically activated bio-oxidised refractory flotation gold concentrates. *Powder Technol.* **2018**, *331*, 258–269. [CrossRef]
19. Asamoah, R.K.; Skinner, W.; Addai-Mensah, J. Pulp mineralogy and chemistry, leaching and rheological behaviour relationships of refractory gold ore dispersions. *Chem. Eng. Res. Des.* **2019**, *146*, 87–103. [CrossRef]
20. Asamoah, R.K.; Zanin, M.; Gascooke, J.; Skinner, W.; Addai-Mensah, J. Refractory gold ores and concentrates part 1: Mineralogical and physico-chemical characteristics. *Miner. Process. Extr. Metall.* **2019**, *129*, 1–13. [CrossRef]
21. Asamoah, R.K.; Zanin, M.; Skinner, W.; Addai-Mensah, J. Refractory gold ores and concentrates part 2: Gold mineralisation and deportment in flotation concentrates and bio-oxidised products. *Miner. Process. Extr. Metall.* **2019**, *129*, 1–14. [CrossRef]
22. Asamoah, R.K. EDTA-enhanced cyanidation of refractory bio-oxidised flotation gold concentrates. *Hydrometallurgy* **2020**, *193*, 1–10. [CrossRef]
23. Asamoah, R.K.; Skinner, W.; Addai-Mensah, J. Enhancing gold recovery from refractory bio-oxidised gold concentrates through high intensity milling. *Miner. Process. Extr. Metall. Trans. Inst. Min. Metall.* **2019**, *129*, 1–10. [CrossRef]
24. Senanayake, G.; Jayasekera, S.; Bandara AM, T.S.; Koenigsberger, E.; Koenigsberger, L.; Kyle, J. Rare earth metal ion solubility in sulphate-phosphate solutions of pH range −0.5 to 5.0 relevant to processing fluorapatite rich concentrates: Effect of calcium, aluminium, iron and sodium ions and temperature up to 80 °C. *Miner. Eng.* **2016**, *98*, 169–176. [CrossRef]
25. Dutrizac, J.E.; Chen, T.T. The behaviour of phosphate during jarosite precipitation. *Hydrometallurgy* **2010**, *102*, 55–65. [CrossRef]
26. Nazari, B.; Jorjani, E.; Hani, H.; Manafi, Z.; Riahi, A. Formation of jarosite and its effect on important ions for Acidithiobacillus ferrooxidans bacteria. *Trans. Nonferrous Met. Soc. China* **2014**, *24*, 1152–1160. [CrossRef]
27. Sadowski, Z. Adhesion of microorganism cells and jarosite particles on the mineral surface. In *Process Metallurgy*; Amils, R., Ballester, A., Eds.; Elsevier: Madrid, Spain, 1999; pp. 393–398.

28. Sasaki, K.; Konno, H. Morphology of jarosite-group compounds precipitated from biologically and chemically oxidized Fe ions. *Can. Mineral.* **2000**, *38*, 45–56. [CrossRef]

29. Miller, P.; Brown, A.R.G. Bacterial oxidation of refractory gold concentrates. In *Gold Ore Processing—Project Development and Operations*; Adams, M.D., Ed.; Elsevier: Amsterdam, The Netherlands, 2016; pp. 359–372.

30. Cathro, K.J.; Koch, D.F.A. The dissolution of gold in cyanide solutions—an electrochemical study. In Proceedings of the Annual Conference of Australasian Institute of Mining and Metallurgy, Western Australia, Australia, 17–22 August 1964.

31. Lorenzen, L. A fundamental study of the dissolution of gold from refractory ores. In *Chemical and Metallurgical Engineering*; University of Stellenbosch: Stellenbosch, South Africa, 1992; p. 329.

32. Aghamirian, M.M.; Yen, W.T. Mechanisms of galvanic interactions between gold and sulfide minerals in cyanide solution. *Miner. Eng.* **2005**, *18*, 393–407. [CrossRef]

33. Dai, X.; Jeffrey, M.I. The effect of sulfide minerals on the leaching of gold in aerated cyanide solutions. *Hydrometallurgy* **2006**, *82*, 118–125. [CrossRef]

34. Azizi, A.; Petre, C.F.; Olsen, C.; Larachi, F. Electrochemical behavior of gold cyanidation in the presence of a sulfide-rich industrial ore versus its major constitutive sulfide minerals. *Hydrometallurgy* **2010**, *101*, 108–119. [CrossRef]

35. Bas, A.D.; Gavril, L.; Zhang, W.; Ghali, E.; Choi, Y. Electrochemical dissolution of roasted gold ore in cyanide solutions. *Hydrometallurgy* **2015**, *156*, 188–198. [CrossRef]